Simulating hearing loss with a transmission-line model for the optimization of hearing aids

PETER VAN HENGEL*

INCAS³, Assen, The Netherlands

Modern hearing aids provide many parameters that can be adjusted to optimize the hearing experience of the individual user. Optimization of these parameters can be based on a comparison of an internal representation of sound processed by the hearing aid and the impaired hearing system with the representation in a non-impaired ear. Models that can represent the most common types of hearing loss and can be adjusted to fit individual hearing loss can play a crucial role in such optimization procedures. Simulations are presented that show the potential of a transmission line model in such a procedure. The model is extended to remap cochleogram energy based on estimations of the local instantaneous frequency. This 'remapping' of the cochleogram gives an advantage in tone-in-noise detection that may be related to neural deafferentation.

INTRODUCTION

Modern hearing aids often contain multiple listening programs for different situations. Each of these programs contains a multitude of parameters that can be adjusted. Finding optimal values for all these parameters often requires more time than is available in a clinical setting of, e.g., an audiological center. To facilitate the optimization process most manufacturers offer first fit settings. Based on the feedback from the user, parameters are adjusted to arrive at an individualized setting. Several contributions in these proceedings address the difficulties in arriving at optimal, or even satisfactory, settings in this manner (e.g., Edwards, 2015).

As described by Biondi (1978), computational models can play an important role in the optimization of parameters in a first fit procedure by simulating the effects of hearing impairment. As shown in Fig. 1, the use of such a computational model allows the comparison of the internal representation of a sound in a normal hearing ear (top path) with the internal representation of the same sound processed first by a hearing aid (prosthesis) and then by a hearing impaired ear.

Optimization of the parameter set (P) of the hearing aid now can be formulated as

$$P_{opt} = \arg\min \varepsilon_2 \qquad \text{(Eq. 1)}$$

where ε_2 is some difference measure. The parameter set P_{opt} that minimizes this distance gives the optimal setting of the hearing aid.

*Corresponding author: petervanhengel@incas3.eu

Proceedings of ISAAR 2015: Individual Hearing Loss – Characterization, Modelling, Compensation Strategies. 5th symposium on Auditory and Audiological Research. August 2015, Nyborg, Denmark. Edited by S. Santurette, T. Dau, J. C. Dalsgaard, L. Tranebjærg, and T. Andersen. ISBN: 978-87-990013-5-4. The Danavox Jubilee Foundation, 2015.

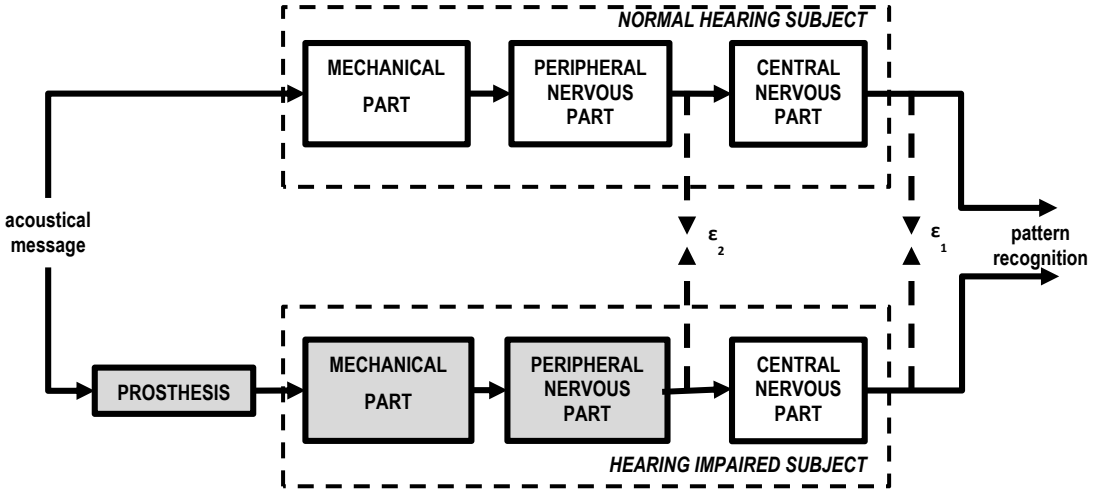

Fig. 1: Block diagram for an optimization procedure for first settings of hearing aids. Adapted from fig 2 of Biondi (1978). The top branch shows the processing of sound in a normal hearing model, the bottom branch in a hearing impaired model with hearing aid. Shaded parts indicate differences with the normal hearing model.

Numerous nonlinear cochlea models have been developed for normal hearing (reviewed, e.g., by Lopez-Poveda, 2005) that could be used. Many of these models offer the possibility to generate internal representations and include options for modelling cochlear hearing loss. Most are implemented as strictly one-way processing. This implies that they do not offer the possibility to simulate otoacoustic emissions (OAEs). Since OAEs are expected to provide essential objective information about active processing in the cochlea the present study uses a transmission-line cochlea model. This model was originally described by Duifhuis *et al.* (1985) and has been used to simulate a variety of physiological and psychoacoustic data (e.g., Epp *et al.*, 2010).

METHODS

Model parameter settings

The parameter settings were taken from Epp *et al.* (2010), including the Greenwood place-frequency map, the Zweig-impedance function (Zweig, 1991) with 1% roughness in the stiffness term and a double Boltzmann nonlinearity in the damping term *d* as well as the delayed feedback stiffness term *s'* (see Epp *et al.*, 2010, for details).

Types of hearing loss simulated

Initially, two types of hearing loss were considered:

- a loss of mechanical to neural conversion, referred to as type I loss;
- a loss of cochlear amplification, referred to as type II loss.

Type I loss was implemented by multiplication of the simulated cochlear partition excitation with an attenuation factor:

$$\vartheta(x) = 1 - D\, e^{-\left(\frac{x-0.5}{0.1}\right)^2} \qquad \text{(Eq. 2)}$$

where x is the relative (longitudinal) distance along the cochlea.

Equation 2 describes an attenuation or loss factor ϑ varying as a function of the (scaled) cochlear length x. In this case, the loss is centred at half of the cochlear length and has a width corresponding to 10% of the cochlear length. Only the depth D is varied in the simulations.

Type II loss was implemented by regarding the nonlinear damping d and feedback stiffness s' (see Epp *et al.*, 2010, for details) as a combination of a passive linear part and an active nonlinear part.

$$d = (1 - \vartheta(x))\, d_{NL} + \vartheta(x)\, d_L \qquad \text{(Eq. 3)}$$

$$s' = (1 - \vartheta(x))\, s'_{NL} \qquad \text{(Eq. 4)}$$

with $\vartheta(x)$ as in Eq. 2.

An additional stage was added to the output of the model. Following the work of Violanda *et al.* (2009), the phase information of the cochlear partition movement was used to extract the local instantaneous frequency at each oscillator in each time frame. Instead of the phase extraction method described in their work, zero crossings of both velocity and displacement were used to estimate local instantaneous frequencies. No correction for group delay was made. Excitation values were remapped to oscillators with resonance frequencies that were closest to the local instantaneous frequencies that were found. A third type of hearing loss – type III loss – could now be simulated, consisting of a loss of this 'remapping' stage.

Output measures

Three types of output were generated from the model to simulate data that can be obtained from hearing impaired subjects in a clinical setting:

- pure tone audiograms;
- distortion-product OAE (DPOAE) levels;
- tone-in-noise detection thresholds.

The pure tone audiograms were computed by comparing the excitation – in the case of loss of mechanical to neural conversion after attenuation – for a 50-ms sinusoid with a 20-ms rising window, to a fixed threshold 3 dB above the excitation for a normal-hearing model without roughness. An iterative procedure was used to find the level of the sinusoid required to match the threshold within 1 dB. Thresholds were computed for frequencies from 500 Hz to 8 kHz using 50 points per octave.

Previous work on simulating hearing loss using the transmission line cochlea model indicated that DPOAE levels were affected by simulated hearing loss (Mauermann *et al.*, 1999). Therefore, DPOAE levels were computed with a simulated probe in the ear canal for the $2f_1$-f_2 component in the range from 500 Hz to 8 kHz using 50 points per octave. The primary levels were at 20 dB and f_2/f_1 was fixed at 1.2.

Tone-in-noise detection thresholds were computed by adding the 50-ms sinusoids (as used for the pure tone audiograms) to a 50 ms snippet of the threshold equalizing noise (TEN, Moore *et al.*, 2000) at a fixed level of 60 dB. Detection thresholds were set at 4 standard deviations above the average noise level, where mean and standard deviations were computed for each oscillator over 50 random 50-ms snippets of the noise. An iterative procedure was used to find signal to noise levels required to match the threshold within 0.1 dB.

RESULTS

Figure 2 shows the pure tone audiograms for simulated loss of type I using values for *D* of 0, 20%, and 100%. The fact that thresholds are found for all frequencies with *D*=100% is due to off-frequency listening. No DPOAEs or tone in noise detection thresholds were calculated for this type of loss, since neither will be affected by an attenuation of the excitation profiles.

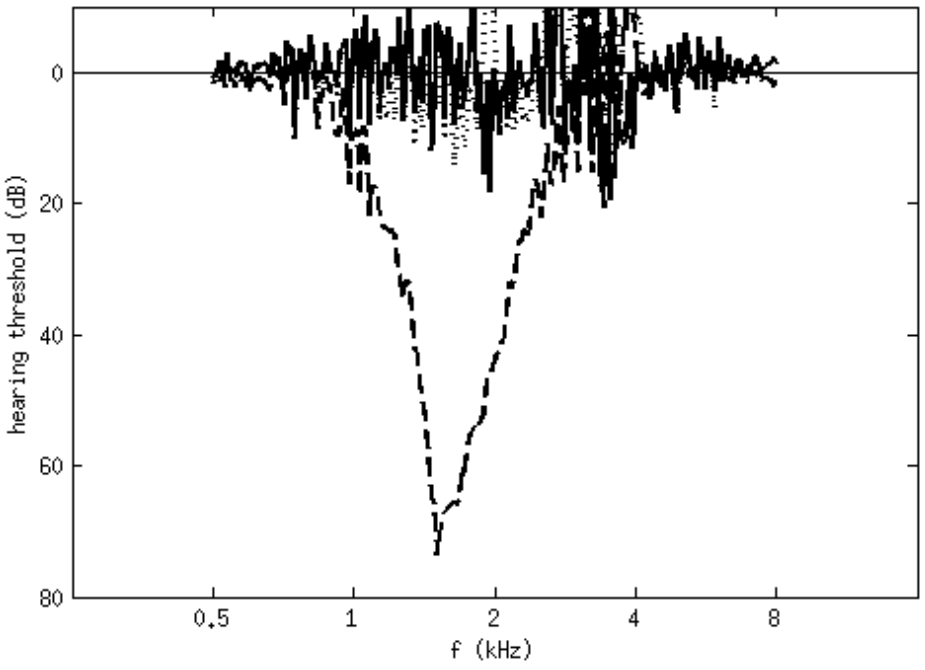

Fig. 2: Pure tone thresholds for type I loss. *D*=0 (solid line), *D*=20% (dotted line), and *D*=100% (dashed line).

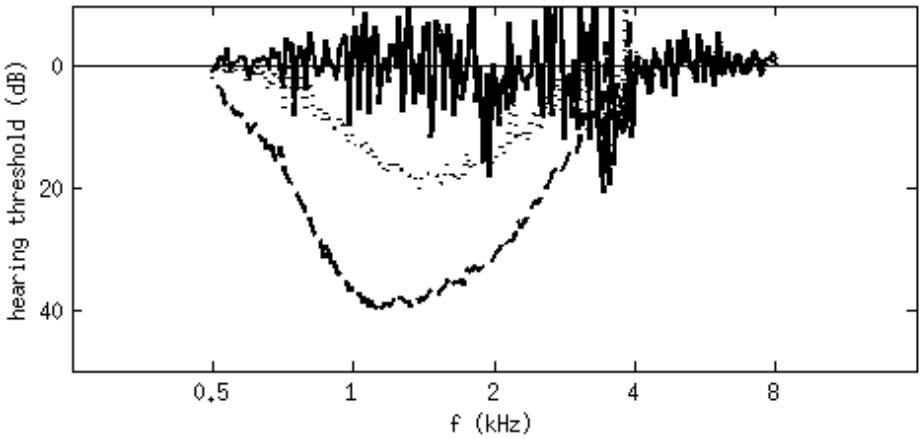

Fig. 3: Pure tone thresholds for type II loss. *D*=0 (solid line), *D*=20% (dotted line), and *D*=100% (dashed line).

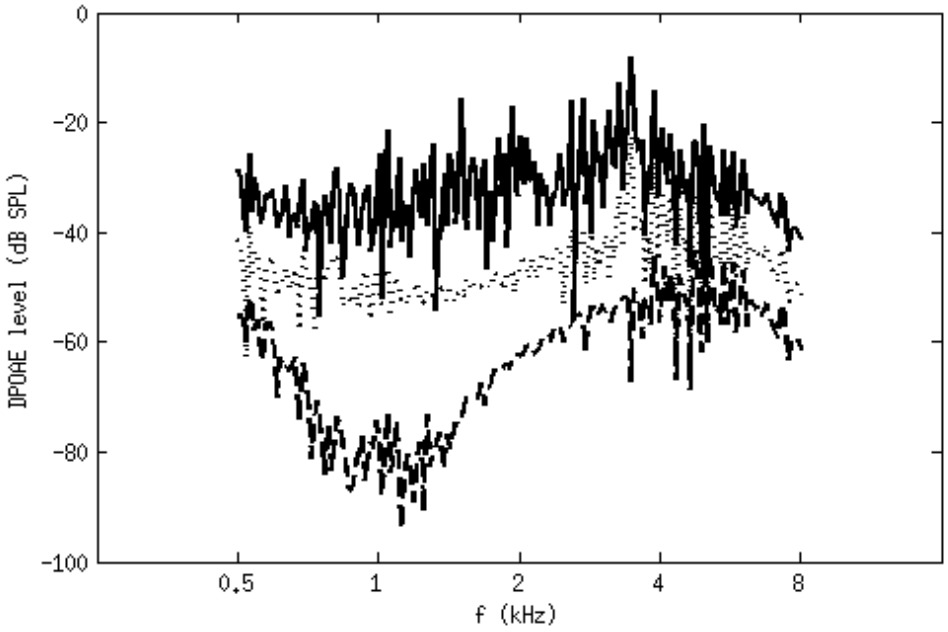

Fig. 4: $2f_1$-f_2 DPOAE levels for type II loss. *D*=0 (solid line), *D*=20% (dotted line), and *D*=100% (dashed line). Lines for *D*=20% and *D*=100% are offset by −10 dB and −20 dB respectively for reasons of clarity.

The curve for no loss (0%) shows threshold fine structure, as is expected from a model with Zweig impedance and roughness (see Epp *et al.*, 2010). At 20% loss the fine structure changes slightly but there is no overall level effect. At 100% loss, the threshold overall level and fine structure are affected, as expected.

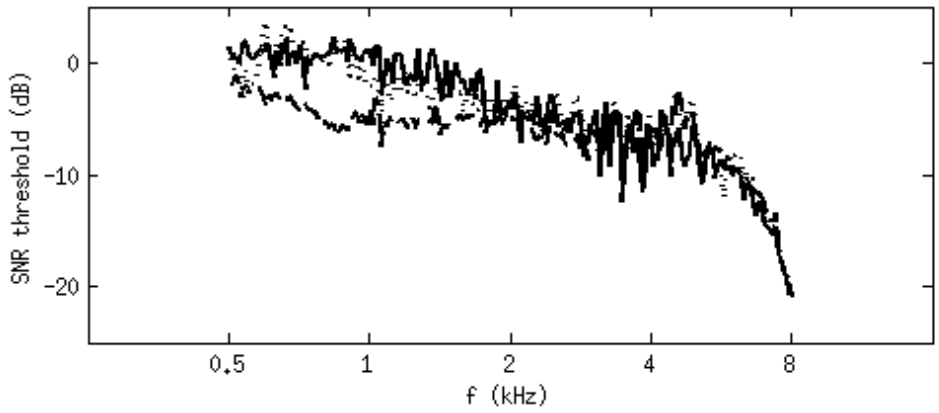

Fig. 5: Tone-in-noise detection thresholds for type II loss. *D*=0 (solid line), *D*=20% (dotted line), and *D*=100% (dashed line).

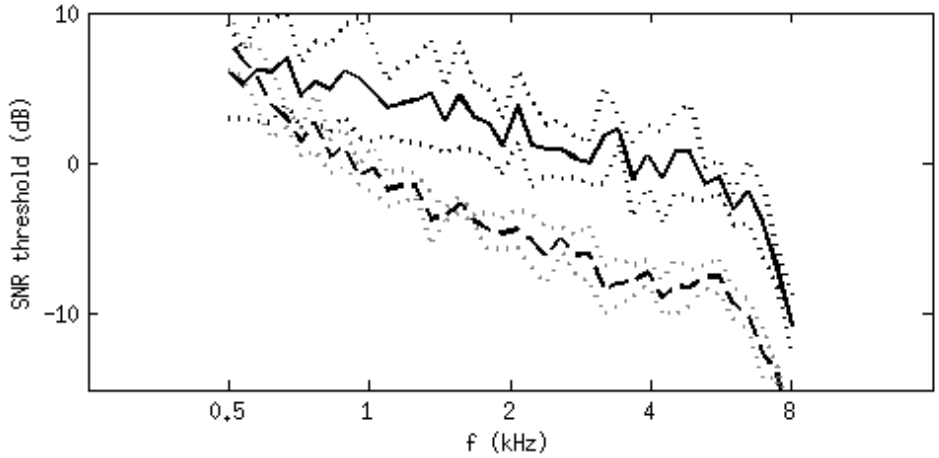

Fig. 6: Tone-in-noise detection thresholds based on excitation profiles without remapping (solid line) and with frequency remapping (dashed line). 20 repetitions were computed for each of the curves showing the mean. Dashed lines indicate standard deviations relative to the mean.

Figures 3, 4, and 5 show the pure tone audiogram, DPOAE levels, and tone-in-noise de-tection thresholds, respectively for simulated loss of type II, using the same values for *D*. As in Fig. 2, the line for no loss (0%) shows fine structure in all three figures.

Figure 3 shows that 20% and 100% loss in terms of pure tone detection results in a reduction in the fine structure and an overall level effect. The maximum loss is approximately 40 dB, which corresponds to the amplification caused by the Zweig impedance function.

Figure 4 shows that the effect of the simulated type II loss on DPOAEs is a loss of fine structure and an overall decrease in level, centred at the $2f_1$-f_2 location and the f_2 location, respectively, as was also found in Mauermann *et al.* (1999).

Figure 5 shows only a limited effect of simulated type II loss on tone-in-noise detection thresholds. Only for 100% loss there is a loss of fine structure and a decrease in thresholds. This contradicts the view that loss of OHC amplification causes difficulties with detection of signals in noise.

Finally, Fig. 6 shows the tone-in-noise detection thresholds based on excitation profiles as computed without and with frequency remapping based on local instantaneous frequencies. In Fig. 5, the same noise snippet was used for all calculations. Because there is a dependence of the choice of noise snippet on the resulting threshold, in this case, 20 repetitions were computed for each frequency and Fig. 6 gives means and standard deviations based on these 20 repetitions. The thresholds after remapping are clearly lower, indicating that the remapping process focusses the tone energy in a single frequency channel, whereas the noise energy remains distributed, making the tone easier to detect.

DISCUSSION

It can be seen from Fig. 2 that small amounts of type I loss will be difficult to detect. Only the curve for the complete loss (100%) shows values that differ significantly from the normal hearing curve. The pure tone audiograms in Fig. 3, and especially the DPOAE levels in Fig. 4 clearly show the effect of a type II loss. Already at 20% loss, a substantial reduction in the fine structure can be observed, as well as a level effect. Since DPOAE levels are relatively easy to measure in a clinical setting, the parameters for type II losses can be easily fitted to individual ears. The tone-in-noise detection thresholds in Fig. 5 hardly show any effect of type II loss, which was one of the reasons to implement type III loss, as described in the Methods section. Only results for the situation without and with remapping were compared.

Figure 6 showed that the remapping of energy provided an improvement in the detection thresholds of about 6 dB for frequencies above 1 kHz. The observation that the improvement was less at the lower frequencies may be due to the relatively short duration of the probe tones. The fact that type III loss did not affect pure tone thresholds or DPOAEs, together with results indicating that deafferentation is associated with a loss of temporal information at the first stages of neural processing, suggests that remapping may occur in the auditory system and a loss of remapping may be the cause of a ‘hidden hearing loss’.

CONCLUSIONS

The transmission line model can be used to simulate three types of hearing loss, associated with loss of mechanical to neural transduction, loss of amplification, and loss of neural coding temporal accuracy. Linking these types of losses to specific damage of hair cells or synapses is difficult since model parameters do not directly relate to structures in the cochlea. In particular, the relation between the Zweig-

impedance function's negative damping and delayed feedback force as well as the electromotility of outer hair cells in the 3D geometry of the organ of Corti are far from clear yet.

However, for the purpose of optimizing hearing aid settings as described by Biondi (1978), a direct link to specific damage in the cochlea may not be required. If the parameters describing the hearing loss can be accurately estimated, the model properly represents the impaired hearing system. This may provide a sufficient base for the optimization procedure in Eq. 1.

REFERENCES

Biondi, E. (**1978**). "Auditory processing of speech and its implications with respect to prosthetic rehabilitation. The bioengineering viewpoint," Audiology, **17**, 43-50.

Duifhuis, H., Hoogstraten, H.W., van Netten, S.M., Diependaal, R.J., and Bialek, W. (**1985**). "Modelling the cochlear partition with coupled Van der Pol oscillators," in *Peripheral Auditory Mechanisms.* Eds. J.B. Allen, J.L. Hall, A.E. Hubbard, S.T. Neely, and A. Tubis (Springer, New York), pp. 290-297.

Edwards, B., (**2015**). "Individualizing hearing aid fitting through novel diagnostics and self-fitting tools," in Proceedings of ISAAR 2015: *Individual hearing loss – Characterization, modelling, compensation strategies*. 5th International Symposium on Auditory and Audiological Research, Nyborg, Denmark. Eds. S. Santurette, T. Dau, J. C. Dalsgaard, L. Tranebjærg, and T. Andersen, The Danavox Jubilee Foundation.

Epp, B., Verhey, J.L., and Mauermann, M. (**2010**). "Modeling cochlear dynamics: Interrelation between cochlea mechanics and psychoacoustics," J. Acoust. Soc. Am., **128**, 1870-1883.

Lopez-Poveda, E.A. (**2005**). "Spectral processing by the peripheral auditory system: facts and models." Int. Rev. Neurobiol., **70**, 7-48.

Mauermann, M., Uppenkamp, S., van Hengel, P.W.J., and Kollmeier, B. (**1999**). "Evidence for the distortion product frequency place as a source of DPOAE fine structure in humans II. Fine structure for different shapes of cochlear hearing loss," J. Acoust. Soc. Am., **106**, 3484-3491.

Moore, B.C., Huss, M., Vickers, D.A., Glasberg, B.R., and Alcántara, J.I. (**2000**). "A test for the diagnosis of dead regions in the cochlea," Br. J. Audiol., **34**, 205-224.

Violanda, R.R., van de Vooren, H., van Elburg, R.A.J., and Andringa, T.C. (**2009**). "Signal component estimation in background noise," Proc. NAG/DAGA 2009, **347**, 1588-1591.

Zweig, G. (**1991**). "Finding the impedance of the organ of Corti," J. Acoust. Soc. Am., **89**, 1229-1254.